Acta Cryst E CRYSTALLOGRAPHIC COMMUNICATIONS

ISSN 2056-9890

Synthesis, crystal structure and Hirshfeld surface analysis of 3-(4-fluorophenyl)-2-formyl-7-methyl-imidazo[1,2-*a*]pyridin-1-ium chloride monohydrate

Firudin I. Guseinov,[a,b] Viacheslav O. Ovsyannikov,[b,c] Pavel V. Sokolovskiy,[b] Yurii L. Sebyakin,[c] Aida I. Samigullina,[b] Mehmet Akkurt,[d] Sevim Türktekin Çelikesir[e] and Ajaya Bhattarai[f]*

[a]Kosygin State University of Russia, 117997 Moscow, Russian Federation, [b]N. D. Zelinsky Institute of Organic Chemistry, Russian Academy of Sciences, 119991 Moscow, Russian Federation, [c]MIREA, Russian Technology University, Lomonosov Institute of Fine Chemical Technology, Moscow 119571, Russian Federation, [d]Department of Physics, Faculty of Sciences, Erciyes University, 38039 Kayseri, Türkiye, [e]Department of Physics, Faculty of Science, Erciyes University, 38039 Kayseri, Türkiye, and [f]Department of Chemistry, M.M.A.M.C. (Tribhuvan University), Biratnagar, Nepal. *Correspondence e-mail: ajaya.bhattarai@mmamc.tu.edu.np

Received 25 July 2023
Accepted 18 August 2023

Edited by J. Reibenspies, Texas A & M University, USA

Keywords: crystal structure; imidazo[1,2-a]pyridin-1-ium; hydrogen bonds; π–π interactions; Hirshfeld surface analysis.

CCDC reference: 2289534

Supporting information: this article has supporting information at journals.iucr.org/e

In the title salt, $C_{15}H_{12}FN_2O^+\cdot Cl^-\cdot H_2O$, the imidazo[1,2-*a*]pyridin-1-ium ring system of the cation is almostly planar [maximum deviaition = −0.047 (2) Å for the ring C atom with the attached arene ring] and forms a dihedral angle of 61.81 (6)° with the plane of the fluorophenyl ring. In the crystal, water molecules form an $R_2^4(8)$ motif parallel to the (100) plane by bonding with the chloride ions *via* O—H···Cl hydrogen bonds. The cations are connected along the *b* axis *via* N—H···O hydrogen bonds involving the O atoms of water molecules, and C—H···O, C—H···Cl and π–π interactions [centroid-to-centroid distance = 3.6195 (8) Å] form layers parallel to the (100) plane. Furthermore, these layers are connected *via* π–π interactions [centroid-to-centroid distance = 3.8051 (9) Å] that further consolidate the crystal structure.

1. Chemical context

Imidazo[1,2-*a*]pyridine is considered to be the most important derivative in the imidazopyridine system, with many important biological activities (Ribeiro *et al.*, 1998; Khalilov *et al.*, 2021). These derivatives exhibit a number of interesting properties, such as anticancer, antifungal, anti-inflammatory, antibacterial, antiprotozoal, antipyretic and anti-infective, as well as analgesic and pain relief and sedative properties (Ribeiro *et al.*, 1998; Almirante *et al.*, 1965; Safavora *et al.*, 2019). Imidazo[1,2-*a*]pyridine is present in various pharmaceutical products, such as zolpidem (used to treat insomnia), alpidem (sedative) (Lacerda *et al.*, 2014), zolimidine (used to treat peptic ulcers) (Tyagi *et al.*, 2012; Martins *et al.*, 2017), olprinone (acute heart failure), saripidem (sedative), necopidem (sedative), soraprazan, miroprofen and minodronic acid (Kielesiński *et al.*, 2015). Due to its importance in the pharmaceutical industry, much effort has been devoted to this heterocycle in order to develop an efficient, feasible and low-cost synthesis of imidazo[1,2-*a*]pyridine derivatives (Ribeiro *et al.*, 1998). Besides their biological activity, the transition-metal complexes of imidazole ligands have been found to possess a wide variety of functional properties, for example, as catalysts, supramolecular building blocks, analytical reagents, *etc.* (Gurbanov *et al.*, 2020*a*,*b*; Kopylovich *et al.*, 2011; Mahmudov *et al.*, 2010, 2012). By the functionalization of the imidazole synthon their functional properties can be improved (Gurbanov *et al.*, 2022; Mahmoudi *et al.*, 2017*a*,*b*, 2019). In

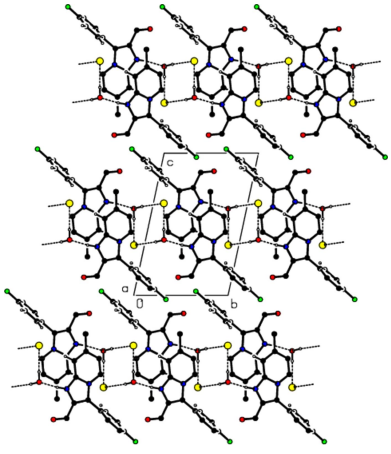

Table 1
Hydrogen-bond geometry (Å, °).

D—H···A	D—H	H···A	D···A	D—H···A
N1—H1···O18^{i}	0.91 (2)	1.77 (2)	2.6754 (16)	174 (2)
O18—H18A···Cl1^{ii}	0.87 (2)	2.24 (2)	3.1070 (11)	175 (2)
O18—H18B···Cl1^{iii}	0.87 (2)	2.24 (2)	3.1142 (11)	178.0 (19)
C8—H8···Cl1^{iv}	0.95	2.69	3.6431 (15)	176
C12—H12···Cl1^{v}	0.95	2.71	3.5610 (16)	150
C13—H13···O10^{vi}	0.95	2.41	3.057 (2)	125

Symmetry codes: (i) $x-1, y, z$; (ii) $x+1, y+1, z$; (iii) $-x+1, -y+1, -z+1$; (iv) $-x, -y+1, -z+1$; (v) $x+1, y, z$; (vi) $x+1, y-1, z$.

addition, the functional groups on the imidazole ring can participate in various types of intermolecular interactions (Mahmudov *et al.*, 2022). Acetal-containing 2-chloro-2-(diethoxymethyl)-3-(4-fluorophenyl)oxirane (**1**) or 1-chloro-3,3-diethoxy-1-(4-fluorophenyl)propan-2-one (**2**) in reactions with bi- and polyfunctional nucleophiles (Fig. 1) turned out to be convenient in the molecular design of various heterocyclic systems, in particular, heterocyclic carbaldehydes and their derivatives (Guseinov *et al.*, 1994, 1995, 1998, 2006, 2017, 2020; Pistsov *et al.*, 2017). We have found that electrophilic reagents (**1** or **2**) react with 2-amino-4-methylpyridine under certain conditions to transform into 3-(4-fluorophenyl)-2-formyl-7-methylimidazo[1,2-*a*]pyridin-1-ium chloride (**3**) whose structure has been determined by NMR spectroscopy and X-ray diffraction methods (Fig. 1).

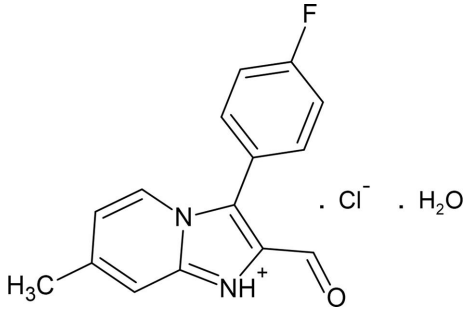

2. Structural commentary

In the title salt (Fig. 2), the imidazo[1,2-*a*]pyridin-1-ium ring system (atoms N1/N4/C2/C3/C5–C8/C8*A*) of the cation is

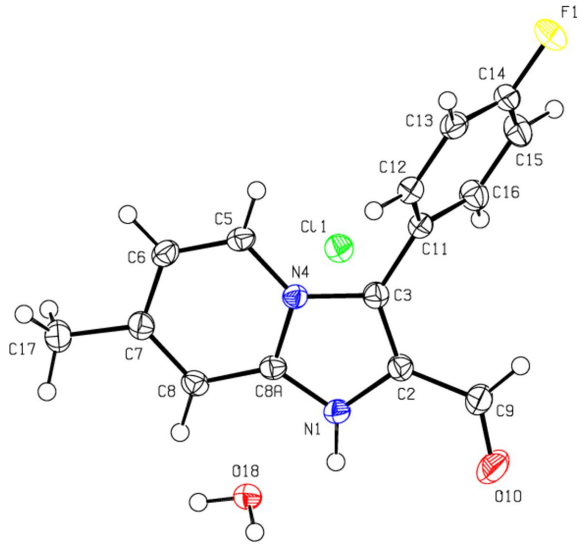

Figure 2
The molecular structure of the title compound, showing the atom labelling and displacement ellipsoids drawn at the 50% probability level.

almost planar [maximum deviaition = −0.047 (2) Å for atom C3] and forms a dihedral angle of 61.81 (6)° with the plane of the fluorophenyl ring (C11–C16).

The bond lengths and angles in the molecule of the title salt are comparable with those of closely related structures detailed in Section 4 (*Database survey*).

3. Supramolecular features and Hirshfeld surface analysis

In the crystal, water molecules form an $R_2^4(8)$ motif (Bernstein *et al.*, 1995) parallel to the (100) plane by bonding with the chloride ions *via* O—H···Cl hydrogen bonds (Table 1 and Figs. 3 and 4). The cations are also connected along the *b* axis *via* N—H···O hydrogen bonds involving the O atoms of the water molecules, and C—H···O, C—H···Cl and π–π interactions [$Cg2\cdots Cg2^{iv}$ = 3.6195 (8) Å; symmetry code: (iv) $-x+1, -y+1, -z+1$; $Cg2$ is a centroid of the six-membered ring (N4/C5–C8/C8*A*) of the imidazo[1,2-*a*]pyridin-1-ium ring system (N1/N4/C2/C3/C5–C8/C8*A*)] form layers parallel to the

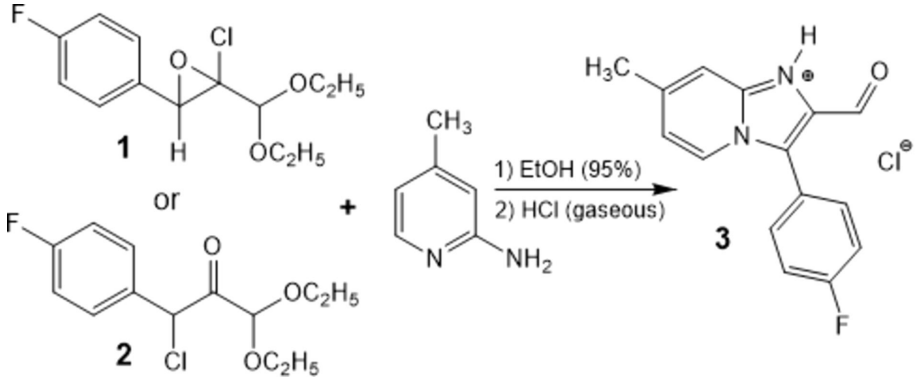

Figure 1
Reaction mechanism of the title compound.

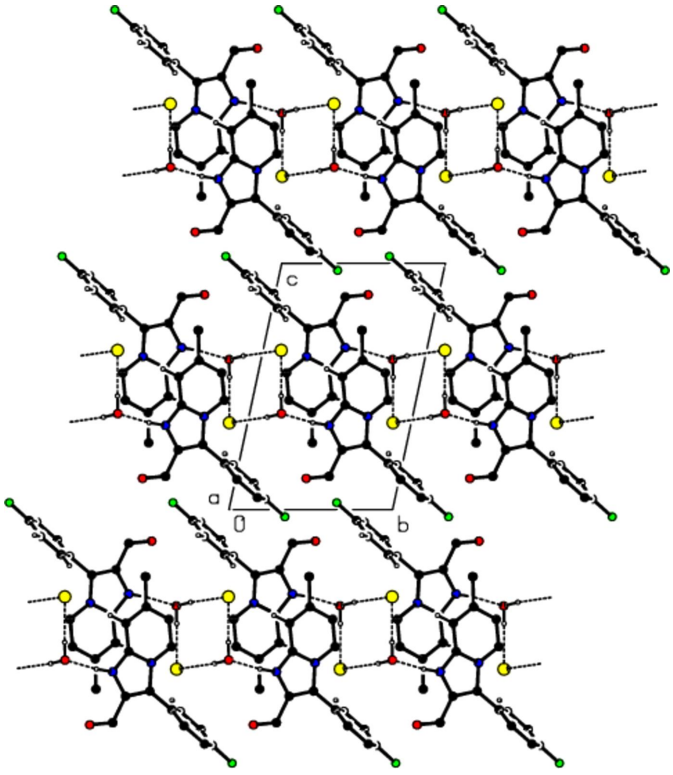

Figure 3
View of the molecular packing along the *a* axis. N—H···O and O—H···Cl hydrogen bonds are shown as dashed lines.

(100) plane (Fig. 5). Furthermore, these layers are connected to each other *via* π–π interactions [$Cg3\cdots Cg3^{vii}$ = 3.8051 (9) Å; symmetry code: (vii) $-x+1, -y, -z+2$; $Cg3$ is a centroid of the fluorophenyl ring (C11–C16)] that consolidate the crystal structure (Fig. 6).

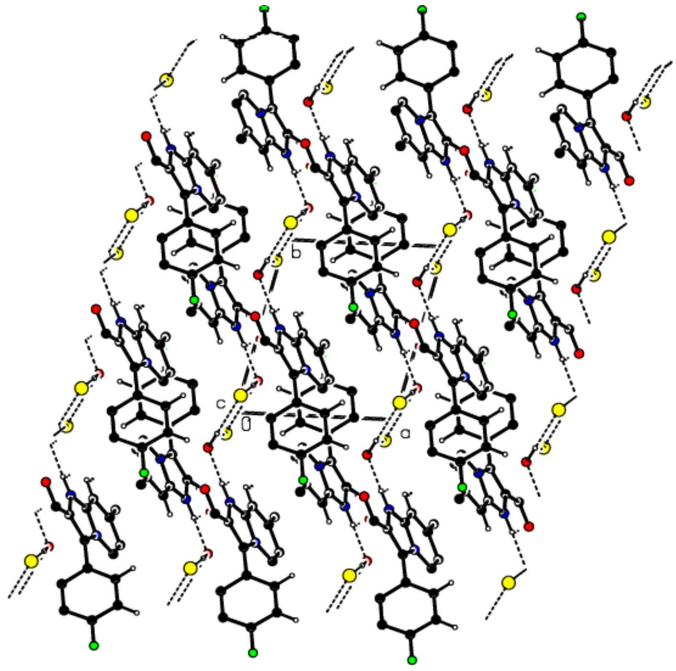

Figure 5
View of the molecular packing along the *c* axis. Hydrogen bonds are depicted as in Fig. 3.

The Hirshfeld surface mapped over d_{norm} was generated using *CrystalExplorer17.5* (Spackman *et al.*, 2021) with a colour scale from −0.7283 a.u. for red to +1.3376 a.u. for blue.

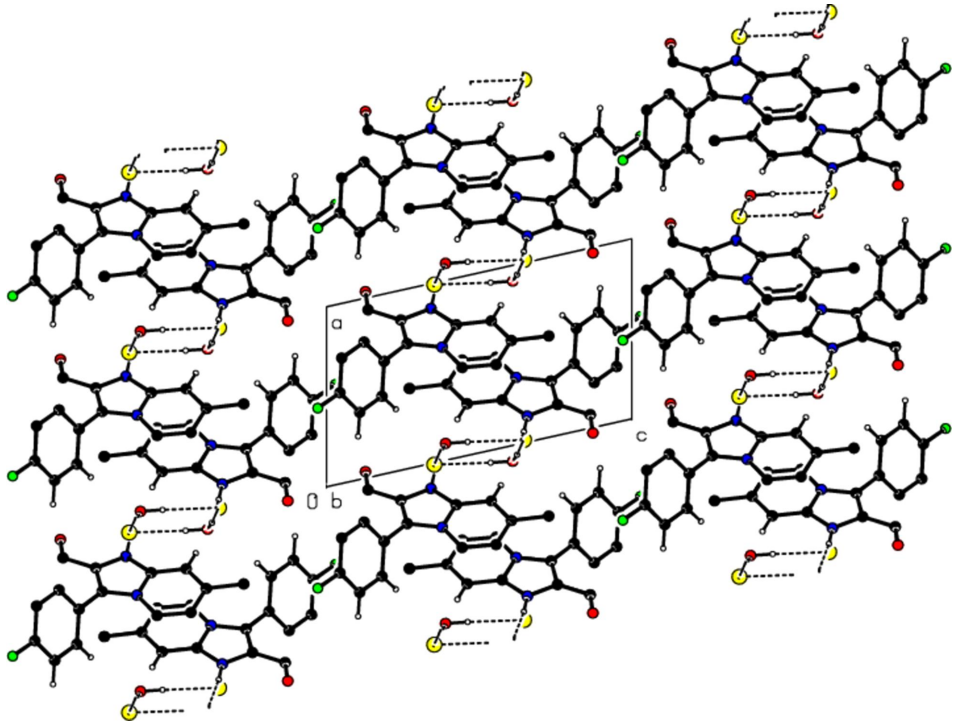

Figure 4
View of the molecular packing along the *b* axis. Hydrogen bonds are depicted as in Fig. 3.

Table 2
Summary of short interatomic contacts (Å) in the title compound.

Contact	Distance	Symmetry operation
H13···O10	2.41	$x+1, y-1, z$
F1···H17*C*	2.78	$x, y-1, z+1$
H9···F1	2.79	$-x+1, -y, -z+2$
H9···O10	2.71	$-x, -y+1, -z+2$
H16···Cl1	3.04	x, y, z
H17*B*···C2	3.02	$-x+1, -y+1, -z+1$
H5···C6	3.02	$-x+1, -y, -z+1$
H17*A*···O18	2.78	$-x+1, -y+1, -z+1$
H8···Cl1	2.69	$-x, -y+1, -z+1$
H15···C9	3.08	$-x, -y, -z+2$
H12···Cl1	2.71	$x+1, y, z$
H5···O18	2.76	$x, y-1, z$
Cl1···H6	2.94	$-x+1, -y, -z+1$
H18*A*···Cl1	2.24	$x+1, y+1, z$
O18···H1	1.77	$x+1, y, z$

The front and rear views of the Hirshfeld surface mapped over d_{norm} are depicted in Fig. 7. The bright-red circular spots on d_{norm} indicate the presence of intermolecular N1—H1···O18^{i}, C8—H8···Cl1^{iv}, C12—H12···Cl1^{v} and C13—H13···O10^{vi} interactions (Table 1). The percentage contributions from different intermolecular interactions towards the formation of a three-dimensional Hirshfeld surface were computed using two-dimensional fingerprint calculations (Fig. 8).

Fig. 8 shows the full two-dimensional fingerprint plots for the molecule and those delineated into the major contacts. H···H interactions [Fig. 8(*b*)] are the major contributor (35.2%) to the crystal packing, with C···H/H···C [Fig. 8(*c*); 19.0%], O···H/H···O [Fig. 8(*d*); 15.5%] and F···H/H···F [Fig. 8(*e*); 9.9%] interactions representing the next highest contributions. The percentage contributions of comparatively weaker interactions are C···C (4.6%), N···H/H···N (2.8%), F···O/O···F (1.5%), Cl···C/C···Cl (1.3%), Cl···H/H···Cl (1.3%), N···C/C···N (1.3%), F···F (1.2%), F···C/C···F (1.1%) and O···O (0.1%). Relevant short intermolecular atomic contacts are summarized in Table 2.

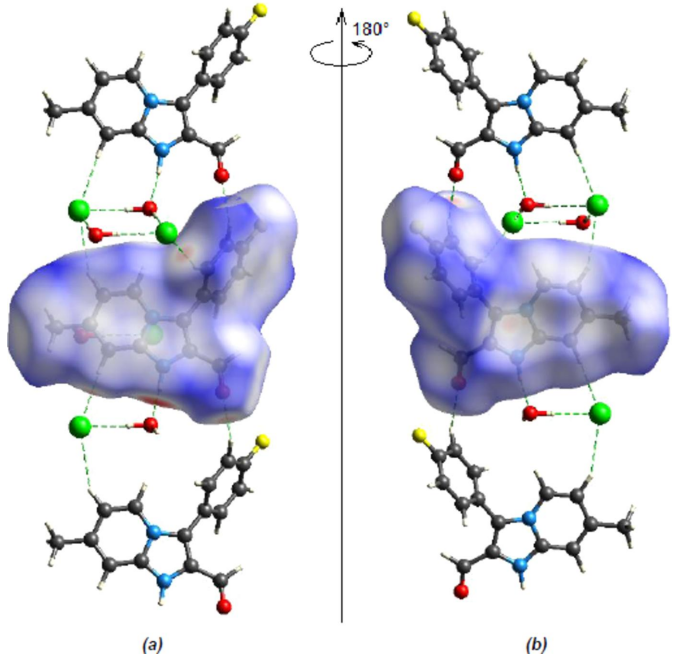

Figure 7
(*a*) Front and (*b*) back sides of the three-dimensional Hirshfeld surface of the title compound mapped over d_{norm}, with a fixed colour scale from −0.7283 to 1.3376 a.u.

The results show that the H···H (35.2%) contacts give the major contribution to the crystal packing, and that the C···H/H···C (19.0%), O···H/H···O (15.5%) and F···H/H···F (9.9%) contacts also give a significant contribution to the total area of the Hirshfeld surface.

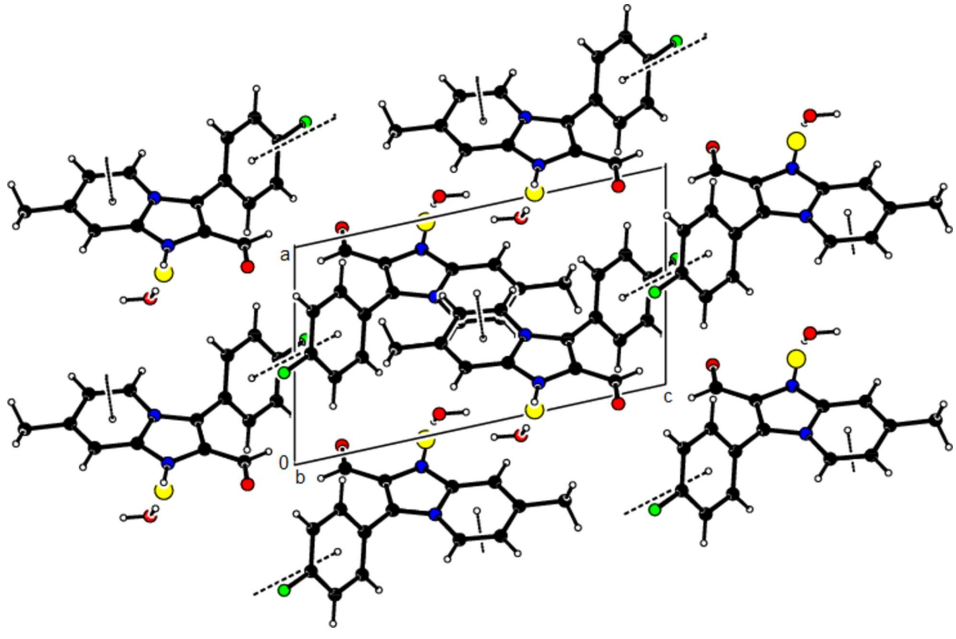

Figure 6
View of the π–π stacking interactions along the *b* axis in the unit cell.

4. Database survey

A search of the Cambridge Structural Database (CSD, Version 5.42, update of September 2021; Groom *et al.*, 2016) for compounds most closely related to the imidazo[1,2-*a*]-pyridin-1-ium unit of the title compound gave the following hits: refcodes LESMAZ (Yin, 2013), UREPIR (Nichol *et al.*, 2011), ABAJOE (Rybakov & Babaev, 2011), BIZWAI02 (Airoldi *et al.*, 2015), UREYIA (Türkyılmaz *et al.*, 2011) and NEQPOP (Qiao *et al.*, 2006).

In the crystal of LESMAZ, the cations and anions are linked into chains parallel to [021] by O—H···Cl and N—H···Cl hydrogen bonds. In the crystal of UREPIR, N—H···O interactions form a one-dimensional chain, which propagates in the *b*-axis direction. C—H···O interactions are also found in the crystal packing. The crystal structure of ABAJOE is consolidated by weak C—H···O and C—H···Cl interactions involving the '*olate*' O atom and the Cl atom attached to the benzoyl group as acceptors. In the crystal of BIZWAI02, molecules are linked by O—H···O, N—H···O and C—H···O hydrogen bonds, and π–π interactions [centroid-to-centroid distance = 3.5822 (11) Å], forming a three-dimensional structure. In the crystal of UREYIA, the components are linked by N—H···O and C—H···O hydrogen bonds and π–π stacking interactions [centroid–centroid separation = 3.642 (3) Å]. In the crystal of NEQPOP, intermolecular O—H···O and N—H···O hydrogen bonds link the molecules into two-dimensional layers.

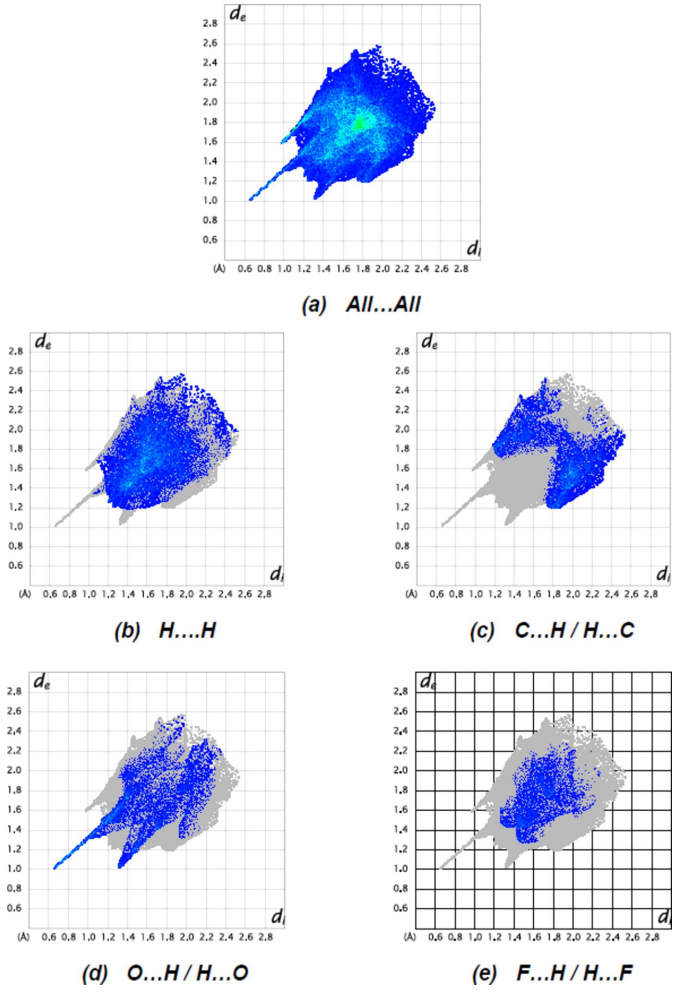

Figure 8
The two-dimensional fingerprint plots of the title compound, showing (*a*) all interactions, and delineated into (*b*) H···H, (*c*) C···H/H···C, (*d*) O···H/H···O and (*e*) F···H/H···F interactions. d_e and d_i represent the distances from a point on the Hirshfeld surface to the nearest atoms outside (external) and inside (internal) the surface, respectively.

Table 3
Experimental details.

Crystal data	
Chemical formula	$C_{15}H_{12}FN_2O^+\cdot Cl^-\cdot H_2O$
M_r	308.73
Crystal system, space group	Triclinic, $P\overline{1}$
Temperature (K)	100
a, *b*, *c* (Å)	7.45681 (13), 8.41737 (10), 12.8928 (2)
α, β, γ (°)	74.0382 (12), 73.7634 (14), 72.7034 (13)
V (Å^3)	725.40 (2)
Z	2
Radiation type	Cu *K*α
μ (mm^{-1})	2.50
Crystal size (mm)	0.33 × 0.19 × 0.15
Data collection	
Diffractometer	Rigaku XtaLAB Synergy Dualflex diffractometer with a HyPix detector
Absorption correction	Gaussian (*CrysAlis PRO*; Rigaku OD, 2023)
T_{min}, T_{max}	0.404, 1.000
No. of measured, independent and observed [$I > 2\sigma(I)$] reflections	15845, 3082, 3033
R_{int}	0.027
(sin $\theta/\lambda)_{max}$ (Å^{-1})	0.634
Refinement	
$R[F^2 > 2\sigma(F^2)]$, $wR(F^2)$, *S*	0.033, 0.086, 1.03
No. of reflections	3082
No. of parameters	203
H-atom treatment	H atoms treated by a mixture of independent and constrained refinement
$\Delta\rho_{max}$, $\Delta\rho_{min}$ (e Å^{-3})	0.34, −0.24

Computer programs: *CrysAlis PRO* (Rigaku OD, 2023), *SHELXT2019* (Sheldrick, 2015*a*), *SHELXL2019* (Sheldrick, 2015*b*), *ORTEP-3 for Windows* (Farrugia, 2012) and *PLATON* (Spek, 2020).

5. Synthesis and crystallization

A solution of equimolar amounts of 2-aminopyridine (410 mg, 3.8 mmol) and 2-chloro-2-(diethoxymethyl)-3-(4-fluorophenyl)oxirane (1) or 1-chloro-3,3-diethoxy-1-(4-fluorophenyl)-propan-2-one (2) (1.05 g, 3.8 mmol) in 25 ml of 95% aqueous ethanol was heated at reflux for 8 h. The solvent was removed *in vacuo*. After purification by column chromatography using a chloroform/ethyl acetate mixture (3:1 *v*/*v*), 2-(diethoxymethyl)-3-(4-fluorophenyl)imidazo[1,2-*a*]pyridine was obtained as a white powder. Gaseous HCl was passed through a solution of 2-(diethoxymethyl)-3-(4-fluorophenyl)imidazo-[1,2-*a*]pyridine in chloroform, leading to the main product, 3-(4-fluorophenyl)-2-formyl-7-methylimidazo[1,2-*a*]pyridin-1-ium chloride (**3**) in the form of a white precipitate; this was

insoluble in chloroform and was filtered off and recrystallized from acetonitrile (Fig. 1). Yield 0.61 g (55%); m.p. 509–510 K. Analysis calculated (%) for $C_{15}H_{12}ClFN_2O$: C 70.58, H 4.74, F 7.44, N 10.97, O 6.27; found: C 70.60, H 4.78, F 7.42, N 10.93, O 6.27. ^{1}H NMR (300 MHz, DMSO-d_6): δ 2.54 (*s*, 3H, CH_3), 7.28 (*d*, *J* = 6.6 Hz, 1H, 6CH), 7.55 (*dd*, *J* = 8.8, 5.5 Hz, 2H, Ar), 7.75 (*s*, 1H, NH), 7.90 (*dd*, *J* = 8.6, 5.5 Hz, 2H, Ar), 8.35 (*s*, 1H, 8CH), 8.47 (*d*, *J* = 7.1 Hz, 1H, 5CH), 9.85 (*s*, 1H, CHO). ^{13}C NMR (200 MHz, DMSO-d_6): δ 21.27, 111.92, 116.44, 116.87, 119.67, 120.02, 126.18, 130.39, 131.39, 133.59 (*d*, *J* = 35 Hz, CF), 141.40, 147.07, 161.11, 166.06, 182.45. ESI–MS: *m*/*z*: 255.0928 $[M + H]^+$.

6. Refinement

Crystal data, data collection and structure refinement details are summarized in Table 3. The N-bound H atom and the H atoms of the water molecule were located in a difference Fourier map and refined freely along with their isotropic displacement parameters. C-bound H atoms were included in calculated positions and treated as riding atoms (C—H = 0.95–0.98 Å), with U_{iso}(H) = 1.2U_{eq}(C) for aromatic H atoms and 1.5U_{eq}(C) for methyl H atoms.

Acknowledgements

The author's contributions are as follows: conceptualization by FIG, MA and AB; synthesis by VOO, PVS, YLS and AIS; X-ray analysis by PVS, AIS and STÇ; writing (review and editing of the manuscript) by FIG, MA and AB; supervision by FIG, MA and AB.

References

Airoldi, A., Bettoni, P., Donnola, M., Calestani, G. & Rizzoli, C. (2015). *Acta Cryst.* E**71**, 51–54.
Almirante, L., Polo, L., Mugnaini, A., Provinciali, E., Rugarli, P., Biancotti, A., Gamba, A. & Murmann, W. (1965). *J. Med. Chem.* **8**, 305–312.
Bernstein, J., Davis, R. E., Shimoni, L. & Chang, N.-L. (1995). *Angew. Chem. Int. Ed. Engl.* **34**, 1555–1573.
Farrugia, L. J. (2012). *J. Appl. Cryst.* **45**, 849–854.
Groom, C. R., Bruno, I. J., Lightfoot, M. P. & Ward, S. C. (2016). *Acta Cryst.* B**72**, 171–179.
Gurbanov, A. V., Kuznetsov, M. L., Demukhamedova, S. D., Alieva, I. N., Godjaev, N. M., Zubkov, F. I., Mahmudov, K. T. & Pombeiro, A. J. L. (2020*a*). *CrystEngComm*, **22**, 628–633.
Gurbanov, A. V., Kuznetsov, M. L., Karmakar, A., Aliyeva, V. A., Mahmudov, K. T. & Pombeiro, A. J. L. (2022). *Dalton Trans.* **51**, 1019–1031.
Gurbanov, A. V., Kuznetsov, M. L., Mahmudov, K. T., Pombeiro, A. J. L. & Resnati, G. (2020*b*). *Chem. Eur. J.* **26**, 14833–14837.
Guseinov, F. I. (1994). *Russ. J. Org. Chem.* **30**, 360–365.
Guseinov, F. I., Pistsov, M. F., Malinnikov, V. M., Lavrova, O. M., Movsumzade, E. M. & Kustov, L. M. (2020). *Mendeleev Commun.* **30**, 674–675.
Guseinov, F. I., Pistsov, M. F., Movsumzade, E. M., Kustov, L. M., Tafeenko, V. A., Chernyshev, V. V., Gurbanov, A. V., Mahmudov, K. T. & Pombeiro, A. J. L. (2017). *Crystals*, **7**, 327.
Guseinov, F. I. & Tagiev, S. Sh. (1995). *Russ. J. Org. Chem.* **31**, 86–91.
Guseinov, F. I. & Yudina, N. A. (1998). *Chem. Heterocycl. Compd.* **34**, 115–120.
Guseinov, F. N., Burangulova, R. N., Mukhamedzyanova, E. F., Strunin, B. P., Sinyashin, O. G., Litvinov, I. A. & Gubaidullin, A. T. (2006). *Chem. Heterocycl. Compd.* **42**, 943–947.
Khalilov, A. N., Tüzün, B., Taslimi, P., Tas, A., Tuncbilek, Z. & Cakmak, N. K. (2021). *J. Mol. Liq.* **344**, 117761.
Kielesiński, Ł., Tasior, M. & Gryko, D. T. (2015). *Org. Chem. Front.* **2**, 21–28.
Kopylovich, M. N., Mahmudov, K. T., Guedes da Silva, M. F. C., Martins, L. M. D. R. S., Kuznetsov, M. L., Silva, T. F. S., Fraústo da Silva, J. J. R. & Pombeiro, A. J. L. (2011). *J. Phys. Org. Chem.* **24**, 764–773.
Lacerda, R. B., Sales, N. M., da Silva, L. L., Tesch, R., Miranda, A. L. P., Barreiro, E. J., Fernandes, P. D. & Fraga, C. A. M. (2014). *PLoS One*, **9**, e91660.
Mahmoudi, G., Dey, L., Chowdhury, H., Bauzá, A., Ghosh, B. K., Kirillov, A. M., Seth, S. K., Gurbanov, A. V. & Frontera, A. (2017*a*). *Inorg. Chim. Acta*, **461**, 192–205.
Mahmoudi, G., Khandar, A. A., Afkhami, F. A., Miroslaw, B., Gurbanov, A. V., Zubkov, F. I., Kennedy, A., Franconetti, A. & Frontera, A. (2019). *CrystEngComm*, **21**, 108–117.
Mahmoudi, G., Zaręba, J. K., Gurbanov, A. V., Bauzá, A., Zubkov, F. I., Kubicki, M., Stilinović, V., Kinzhybalo, V. & Frontera, A. (2017*b*). *Eur. J. Inorg. Chem.* **2017**, 4763–4772.
Mahmudov, K. T., Guedes da Silva, M. F. C., Glucini, M., Renzi, M., Gabriel, K. C. P., Kopylovich, M. N., Sutradhar, M., Marchetti, F., Pettinari, C., Zamponi, S. & Pombeiro, A. J. L. (2012). *Inorg. Chem. Commun.* **22**, 187–189.
Mahmudov, K. T., Gurbanov, A. V., Aliyeva, V. A., Guedes da Silva, M. F. C., Resnati, G. & Pombeiro, A. J. L. (2022). *Coord. Chem. Rev.* **464**, 214556.
Mahmudov, K. T., Maharramov, A. M., Aliyeva, R. A., Aliyev, I. A., Kopylovich, M. N. & Pombeiro, A. J. L. (2010). *Anal. Lett.* **43**, 2923–2938.
Martins, N. M. R., Anbu, S., Mahmudov, K. T., Ravishankaran, R., Guedes da Silva, M. F. C., Martins, L. M. D. R. S., Karande, A. A. & Pombeiro, A. J. L. (2017). *New J. Chem.* **41**, 4076–4086.
Nichol, G. S., Sharma, A. & Li, H.-Y. (2011). *Acta Cryst.* E**67**, o1224.
Pistsov, M. F., Lavrova, O. M., Saifutdinov, A. M., Burangulova, R. N., Kustov, L. M., Guseinov, F. I. & Musin, R. Z. (2017). *Russ. J. Gen. Chem.* **87**, 2887–2890.
Qiao, S., Yong, G.-P., Xie, Y. & Wang, Z.-Y. (2006). *Acta Cryst.* E**62**, o4634–o4635.
Ribeiro, I. G. M., da Silva, K. C., Parrini, S. C., de Miranda, A. L. P., Fraga, C. A. M. & Barreiro, E. J. (1998). *Eur. J. Med. Chem.* **33**, 225–235.
Rigaku OD (2023). *CrysAlis PRO*. Rigaku Oxford Diffraction Ltd, Yarnton, Oxfordshire, England.
Rybakov, V. B. & Babaev, E. V. (2011). *Acta Cryst.* E**67**, o2814.
Safavora, A. S., Brito, I., Cisterna, J., Cárdenas, A., Huseynov, E. Z., Khalilov, A. N., Naghiyev, F. N., Askerov, R. K. & Maharramov, A. M. (2019). *Z. Kristallogr. New Cryst. Struct.* **234**, 1183–1185.
Sheldrick, G. M. (2015*a*). *Acta Cryst.* A**71**, 3–8.
Sheldrick, G. M. (2015*b*). *Acta Cryst.* C**71**, 3–8.
Spackman, P. R., Turner, M. J., McKinnon, J. J., Wolff, S. K., Grimwood, D. J., Jayatilaka, D. & Spackman, M. A. (2021). *J. Appl. Cryst.* **54**, 1006–1011.
Spek, A. L. (2020). *Acta Cryst.* E**76**, 1–11.
Türkyılmaz, M., Baran, Y. & Özdemir, N. (2011). *Acta Cryst.* E**67**, o1282.
Tyagi, V., Khan, S., Bajpai, V., Gauniyal, H. M., Kumar, B. & Chauhan, P. M. S. (2012). *J. Org. Chem.* **77**, 1414–1421.
Yin, W.-Y. (2013). *Acta Cryst.* E**69**, o211.

supporting information

Acta Cryst. (2023). E**79**, 899-904 [https://doi.org/10.1107/S2056989023007272]

Synthesis, crystal structure and Hirshfeld surface analysis of 3-(4-fluorophenyl)-2-formyl-7-methylimidazo[1,2-*a*]pyridin-1-ium chloride monohydrate

Firudin I. Guseinov, Viacheslav O. Ovsyannikov, Pavel V. Sokolovskiy, Yurii L. Sebyakin, Aida I. Samigullina, Mehmet Akkurt, Sevim Türktekin Çelikesir and Ajaya Bhattarai

Computing details

Data collection: *CrysAlis PRO* (Rigaku OD, 2023); cell refinement: *CrysAlis PRO* (Rigaku OD, 2023); data reduction: *CrysAlis PRO* (Rigaku OD, 2023); program(s) used to solve structure: SHELXT2019 (Sheldrick, 2015*a*); program(s) used to refine structure: *SHELXL2019* (Sheldrick, 2015*b*); molecular graphics: *ORTEP-3 for Windows* (Farrugia, 2012); software used to prepare material for publication: *PLATON* (Spek, 2020).

3-(4-Fluorophenyl)-2-formyl-7-methylimidazo[1,2-*a*]pyridin-1-ium chloride monohydrate

Crystal data

$C_{15}H_{12}FN_2O^+\cdot Cl^-\cdot H_2O$
M_r = 308.73
Triclinic, $P\overline{1}$
a = 7.45681 (13) Å
b = 8.41737 (10) Å
c = 12.8928 (2) Å
α = 74.0382 (12)°
β = 73.7634 (14)°
γ = 72.7034 (13)°
V = 725.40 (2) Å^3
Z = 2
$F(000)$ = 320
D_x = 1.413 Mg m^{-3}
Cu $K\alpha$ radiation, λ = 1.54184 Å
Cell parameters from 11896 reflections
θ = 3.6–77.3°
μ = 2.50 mm^{-1}
T = 100 K
Prism, colorless
0.33 × 0.19 × 0.15 mm

Data collection

Rigaku XtaLAB Synergy Dualflex diffractometer with a HyPix detector
Radiation source: micro-focus sealed X-ray tube, PhotonJet (Cu) X-ray Source
Mirror monochromator
Detector resolution: 10.0000 pixels mm^{-1}
ω scans
Absorption correction: gaussian (CrysAlis PRO; Rigaku OD, 2023)
T_{min} = 0.404, T_{max} = 1.000
15845 measured reflections
3082 independent reflections
3033 reflections with $I > 2\sigma(I)$
R_{int} = 0.027
θ_{max} = 77.9°, θ_{min} = 3.7°
h = −9→9
k = −10→9
l = −16→16

Refinement

Refinement on F^2
Least-squares matrix: full
$R[F^2 > 2\sigma(F^2)]$ = 0.033
$wR(F^2)$ = 0.086
S = 1.03
3082 reflections
203 parameters
0 restraints
Primary atom site location: dual
Secondary atom site location: difference Fourier map
Hydrogen site location: mixed

H atoms treated by a mixture of independent and constrained refinement
$w = 1/[\sigma^2(F_o^2) + (0.0415P)^2 + 0.4038P]$ where $P = (F_o^2 + 2F_c^2)/3$

$(\Delta/\sigma)_{max} = 0.001$
$\Delta\rho_{max} = 0.34$ e Å^{-3}
$\Delta\rho_{min} = -0.24$ e Å^{-3}

Special details

Geometry. All esds (except the esd in the dihedral angle between two l.s. planes) are estimated using the full covariance matrix. The cell esds are taken into account individually in the estimation of esds in distances, angles and torsion angles; correlations between esds in cell parameters are only used when they are defined by crystal symmetry. An approximate (isotropic) treatment of cell esds is used for estimating esds involving l.s. planes.

Fractional atomic coordinates and isotropic or equivalent isotropic displacement parameters (Å^2)

	x	*y*	*z*	U_{iso}*/U_{eq}
Cl1	0.01542 (4)	0.11097 (4)	0.64700 (3)	0.02403 (11)
F1	0.56045 (14)	−0.35098 (11)	1.02878 (8)	0.0367 (2)
O18	0.90723 (15)	0.80467 (12)	0.61002 (9)	0.0241 (2)
N4	0.37156 (15)	0.27422 (14)	0.62115 (9)	0.0190 (2)
N1	0.14182 (17)	0.49767 (15)	0.65794 (10)	0.0215 (2)
C8A	0.26290 (18)	0.42655 (16)	0.57537 (11)	0.0196 (3)
C11	0.37885 (19)	0.08741 (17)	0.81151 (11)	0.0210 (3)
C5	0.51012 (19)	0.17210 (16)	0.55569 (12)	0.0214 (3)
H5	0.586532	0.067821	0.587952	0.026*
C12	0.5714 (2)	0.03302 (17)	0.81846 (11)	0.0233 (3)
H12	0.660070	0.098082	0.773040	0.028*
C3	0.30886 (19)	0.24618 (17)	0.73582 (11)	0.0208 (3)
C7	0.4192 (2)	0.37812 (17)	0.39448 (11)	0.0228 (3)
C2	0.16899 (19)	0.38788 (17)	0.75689 (11)	0.0217 (3)
C8	0.28524 (19)	0.48118 (17)	0.46032 (11)	0.0215 (3)
H8	0.209704	0.586666	0.428855	0.026*
C14	0.5015 (2)	−0.20644 (18)	0.95627 (12)	0.0267 (3)
C16	0.2482 (2)	−0.00887 (19)	0.87709 (12)	0.0271 (3)
H16	0.117247	0.027457	0.871462	0.032*
C6	0.5351 (2)	0.22342 (17)	0.44449 (12)	0.0232 (3)
H6	0.631903	0.154967	0.398747	0.028*
C13	0.6343 (2)	−0.11584 (18)	0.89146 (12)	0.0256 (3)
H13	0.765513	−0.154250	0.896619	0.031*
C17	0.4406 (2)	0.4222 (2)	0.27152 (12)	0.0295 (3)
H17A	0.374708	0.355153	0.250243	0.044*
H17B	0.577414	0.396555	0.235805	0.044*
H17C	0.383705	0.543651	0.248116	0.044*
C15	0.3103 (2)	−0.1578 (2)	0.95051 (12)	0.0303 (3)
H15	0.223073	−0.224471	0.995677	0.036*
C9	0.0719 (2)	0.4320 (2)	0.86403 (12)	0.0305 (3)
H9	0.092957	0.349329	0.929217	0.037*
H18A	0.937 (3)	0.887 (3)	0.6243 (19)	0.046 (6)*
H18B	0.926 (3)	0.830 (3)	0.538 (2)	0.045 (6)*
H1	0.059 (3)	0.602 (3)	0.6466 (17)	0.042 (5)*
O10	−0.0336 (2)	0.56891 (18)	0.87279 (11)	0.0572 (4)

Atomic displacement parameters (Å²)

	U^{11}	U^{22}	U^{33}	U^{12}	U^{13}	U^{23}
Cl1	0.02505 (17)	0.02388 (17)	0.02491 (17)	−0.00803 (12)	−0.00593 (12)	−0.00495 (12)
F1	0.0455 (6)	0.0280 (5)	0.0283 (5)	−0.0034 (4)	−0.0120 (4)	0.0055 (4)
O18	0.0284 (5)	0.0197 (5)	0.0241 (5)	−0.0053 (4)	−0.0058 (4)	−0.0045 (4)
N4	0.0200 (5)	0.0177 (5)	0.0196 (5)	−0.0050 (4)	−0.0035 (4)	−0.0047 (4)
N1	0.0221 (5)	0.0188 (5)	0.0217 (6)	−0.0011 (4)	−0.0052 (4)	−0.0050 (4)
C8A	0.0195 (6)	0.0174 (6)	0.0228 (6)	−0.0051 (5)	−0.0046 (5)	−0.0048 (5)
C11	0.0231 (6)	0.0203 (6)	0.0189 (6)	−0.0031 (5)	−0.0039 (5)	−0.0057 (5)
C5	0.0201 (6)	0.0178 (6)	0.0265 (7)	−0.0047 (5)	−0.0032 (5)	−0.0068 (5)
C12	0.0236 (6)	0.0232 (6)	0.0216 (6)	−0.0041 (5)	−0.0030 (5)	−0.0060 (5)
C3	0.0214 (6)	0.0215 (6)	0.0205 (6)	−0.0060 (5)	−0.0045 (5)	−0.0048 (5)
C7	0.0267 (7)	0.0225 (6)	0.0220 (6)	−0.0126 (5)	−0.0023 (5)	−0.0048 (5)
C2	0.0218 (6)	0.0223 (6)	0.0202 (6)	−0.0044 (5)	−0.0047 (5)	−0.0036 (5)
C8	0.0245 (6)	0.0187 (6)	0.0227 (6)	−0.0070 (5)	−0.0064 (5)	−0.0031 (5)
C14	0.0356 (8)	0.0216 (7)	0.0194 (6)	−0.0015 (6)	−0.0077 (6)	−0.0026 (5)
C16	0.0249 (7)	0.0286 (7)	0.0261 (7)	−0.0068 (6)	−0.0051 (5)	−0.0032 (6)
C6	0.0242 (6)	0.0218 (6)	0.0247 (7)	−0.0073 (5)	−0.0006 (5)	−0.0094 (5)
C13	0.0260 (7)	0.0250 (7)	0.0235 (7)	0.0007 (5)	−0.0069 (5)	−0.0075 (5)
C17	0.0375 (8)	0.0301 (7)	0.0219 (7)	−0.0135 (6)	−0.0021 (6)	−0.0054 (6)
C15	0.0330 (8)	0.0305 (8)	0.0244 (7)	−0.0113 (6)	−0.0036 (6)	0.0006 (6)
C9	0.0306 (7)	0.0321 (8)	0.0227 (7)	0.0010 (6)	−0.0039 (6)	−0.0073 (6)
O10	0.0698 (10)	0.0467 (8)	0.0304 (6)	0.0263 (7)	−0.0082 (6)	−0.0152 (6)

Geometric parameters (Å, º)

F1—C14	1.3542 (16)	C7—C8	1.3734 (19)
O18—H18A	0.86 (2)	C7—C6	1.428 (2)
O18—H18B	0.87 (2)	C7—C17	1.4988 (19)
N4—C8A	1.3719 (17)	C2—C9	1.4605 (19)
N4—C5	1.3791 (17)	C8—H8	0.9500
N4—C3	1.3955 (17)	C14—C13	1.377 (2)
N1—C8A	1.3411 (17)	C14—C15	1.379 (2)
N1—C2	1.3811 (17)	C16—H16	0.9500
N1—H1	0.92 (2)	C16—C15	1.389 (2)
C8A—C8	1.4042 (19)	C6—H6	0.9500
C11—C12	1.3920 (19)	C13—H13	0.9500
C11—C3	1.4709 (18)	C17—H17A	0.9800
C11—C16	1.3973 (19)	C17—H17B	0.9800
C5—H5	0.9500	C17—H17C	0.9800
C5—C6	1.354 (2)	C15—H15	0.9500
C12—H12	0.9500	C9—H9	0.9500
C12—C13	1.387 (2)	C9—O10	1.2011 (19)
C3—C2	1.3654 (19)		
H18A—O18—H18B	103 (2)	C8A—C8—H8	120.9
C8A—N4—C5	121.11 (12)	C7—C8—C8A	118.26 (12)

C8A—N4—C3	108.76 (11)	C7—C8—H8	120.9
C5—N4—C3	130.04 (11)	F1—C14—C13	118.85 (13)
C8A—N1—C2	108.37 (11)	F1—C14—C15	118.03 (13)
C8A—N1—H1	123.1 (13)	C13—C14—C15	123.12 (13)
C2—N1—H1	128.5 (13)	C11—C16—H16	120.1
N4—C8A—C8	121.05 (12)	C15—C16—C11	119.86 (13)
N1—C8A—N4	108.00 (11)	C15—C16—H16	120.1
N1—C8A—C8	130.92 (12)	C5—C6—C7	121.48 (12)
C12—C11—C3	121.05 (12)	C5—C6—H6	119.3
C12—C11—C16	120.14 (13)	C7—C6—H6	119.3
C16—C11—C3	118.81 (12)	C12—C13—H13	120.9
N4—C5—H5	120.7	C14—C13—C12	118.22 (13)
C6—C5—N4	118.69 (12)	C14—C13—H13	120.9
C6—C5—H5	120.7	C7—C17—H17A	109.5
C11—C12—H12	119.9	C7—C17—H17B	109.5
C13—C12—C11	120.26 (13)	C7—C17—H17C	109.5
C13—C12—H12	119.9	H17A—C17—H17B	109.5
N4—C3—C11	123.90 (11)	H17A—C17—H17C	109.5
C2—C3—N4	105.71 (11)	H17B—C17—H17C	109.5
C2—C3—C11	130.28 (12)	C14—C15—C16	118.39 (14)
C8—C7—C6	119.34 (13)	C14—C15—H15	120.8
C8—C7—C17	121.11 (13)	C16—C15—H15	120.8
C6—C7—C17	119.51 (13)	C2—C9—H9	118.8
N1—C2—C9	122.80 (12)	O10—C9—C2	122.45 (14)
C3—C2—N1	109.06 (12)	O10—C9—H9	118.8
C3—C2—C9	127.88 (13)		

F1—C14—C13—C12	−179.27 (12)	C12—C11—C3—N4	62.54 (18)
F1—C14—C15—C16	179.42 (13)	C12—C11—C3—C2	−121.88 (16)
N4—C8A—C8—C7	−0.07 (19)	C12—C11—C16—C15	1.0 (2)
N4—C5—C6—C7	−1.2 (2)	C3—N4—C8A—N1	3.08 (14)
N4—C3—C2—N1	1.89 (15)	C3—N4—C8A—C8	−175.22 (12)
N4—C3—C2—C9	−172.39 (14)	C3—N4—C5—C6	175.22 (12)
N1—C8A—C8—C7	−177.93 (13)	C3—C11—C12—C13	179.08 (12)
N1—C2—C9—O10	−2.3 (3)	C3—C11—C16—C15	−178.93 (13)
C8A—N4—C5—C6	−1.22 (18)	C3—C2—C9—O10	171.26 (17)
C8A—N4—C3—C11	173.45 (12)	C2—N1—C8A—N4	−1.87 (15)
C8A—N4—C3—C2	−3.04 (14)	C2—N1—C8A—C8	176.21 (13)
C8A—N1—C2—C3	−0.05 (15)	C8—C7—C6—C5	3.0 (2)
C8A—N1—C2—C9	174.58 (13)	C16—C11—C12—C13	−0.8 (2)
C11—C12—C13—C14	−0.2 (2)	C16—C11—C3—N4	−117.56 (15)
C11—C3—C2—N1	−174.29 (13)	C16—C11—C3—C2	58.0 (2)
C11—C3—C2—C9	11.4 (2)	C6—C7—C8—C8A	−2.29 (19)
C11—C16—C15—C14	−0.1 (2)	C13—C14—C15—C16	−1.0 (2)
C5—N4—C8A—N1	−179.80 (11)	C17—C7—C8—C8A	175.47 (12)
C5—N4—C8A—C8	1.90 (18)	C17—C7—C6—C5	−174.78 (13)
C5—N4—C3—C11	−3.3 (2)	C15—C14—C13—C12	1.2 (2)
C5—N4—C3—C2	−179.83 (13)		

Hydrogen-bond geometry (Å, º)

D—H···*A*	*D*—H	H···*A*	*D*···*A*	*D*—H···*A*
N1—H1···O18^{i}	0.91 (2)	1.77 (2)	2.6754 (16)	174 (2)
O18—H18*A*···Cl1^{ii}	0.87 (2)	2.24 (2)	3.1070 (11)	175 (2)
O18—H18*B*···Cl1^{iii}	0.87 (2)	2.24 (2)	3.1142 (11)	178.0 (19)
C8—H8···Cl1^{iv}	0.95	2.69	3.6431 (15)	176
C12—H12···Cl1^{v}	0.95	2.71	3.5610 (16)	150
C13—H13···O10^{vi}	0.95	2.41	3.057 (2)	125

Symmetry codes: (i) $x-1, y, z$; (ii) $x+1, y+1, z$; (iii) $-x+1, -y+1, -z+1$; (iv) $-x, -y+1, -z+1$; (v) $x+1, y, z$; (vi) $x+1, y-1, z$.